# Finite Element Analysis of the Postbuckling Behavior of Structures

AKIN ECER*
*University of Wisconsin—Milwaukee, Milwaukee, Wis.*

**A unified treatment of the numerical analysis of postbuckling behavior, based on the matrix formulation of structures, is developed. A third-order large displacement analysis is employed to derive the incremental equilibrium equations directly. A perturbation analyses is then performed. The required critical buckling point for different types of structures is obtained from known finite element models. The postbuckling behavior is determined from the direct solution of a system of linear algebraic equations. Numerical results for funicular arches, columns and plates are presented to demonstrate the generality and applicability of the method.**

## I. Introduction

THE systematic analysis of the postbuckling behavior of structures is a relatively recent development of the theory of elastic stability. Koiter[1] has presented a comprehensive high-order theory describing the stability and immediate postbuckling behavior of structures and the effects of imperfections. His work was further extended by Sewell,[2] Thompson,[3] Budiansky and Hutchinson.[4] A direct application of Koiter's theory using the finite element method has been given by Lang[5] based on the discretization of total energy in terms of assumed displacement functions.

The finite element method has also been applied for analyzing the large displacement behavior of slender structures by considering a higher order incremental theory. Development of such formulations has been summarized by Mallett and Marcal[6] and the incremental equilibrium equations were discussed in terms of linear elastic, first- and second-order geometric matrices. Higher order incremental equilibrium equations have also been applied for determining the large displacement behavior of different types of structures in the post-buckling region.[7-9] Applications of incremental equilibrium equations for determining asymptotic postbuckling behavior has been presented by Mau and Gallagher[10] based on the formulation in Ref. 6. These authors have also emphasized the importance of prebuckling deformations in the stability analysis. Another significant attempt for the Koiter type analysis of the postbuckling behavior using finite elements was presented by Haftka et al.,[11] who treated the nonlinear terms as imperfections and analyzed the instability in terms of an imperfect linear structure.

In the presented analysis the incremental large displacement theory is applied for a complete formulation of Koiter's theory by considering first-, second- and third-order geometric stiffness matrices besides the elastic stiffness matrix. The geometric nonlinearities are separated from the element behavior at the beginning of the formulation from which Koiter's theory was developed in terms of the stiffness, loading and geometry of the structure. The important concepts of the theory of elastic stability are also discussed in terms of these parameters which cannot be achieved through direct energy formulation[5] or as presented in the previous applications of incremental equilibrium equations.[10] Another important feature of the analysis is the unification of the linear matrix stability analysis of structures with the analysis of postbuckling behavior and imperfection sensitivity. Since there has been considerable work done in the finite element analysis of linear stability problems, this work will clearly indicate the requirements for a postbuckling analysis as an extension of such developments. The method is formulated in general form for slender elastic structures. It can be applied to different types of structures (arches, plates and shells) for which several finite element models have already been developed for determining the incremental stiffness matrix.

Presented as Paper 73-255 at the AIAA 11th Aerospace Sciences Conference, Washington, D.C., January 10–12, 1973; submitted January 22, 1973; revision received May 3, 1973.

Index category: Structural Stability Analysis.

* Assistant Professor of Engineering Mechanics. Member AIAA.

## II. Finite Element Analysis of Large Displacement and Buckling Problems

The finite element method has been employed in formulating large displacement problems by several authors.[6,12,13] Three different types of force-displacement systems are combined in developing the large displacement, finite element formulation of structures, as shown in Fig. 1. Each of these systems are related by the equilibrium and compatability conditions of the structure as follows. a) The structure is divided into elements, where each element ($g$) has an incremental nodal force displacement system, $(P_i^g - \rho_i^g)$ at the node ($i$). b) For each element a system of $n$ independent incremental generalized stress-strain relationships $(S_i^g - v_i^g)$ are defined, with $n$ depending on the type of the structure. c) A third system is defined for the entire structure by the incremental nodal forces and displacements $(R_i - r_i)$. Using the equilibrium and compatability conditions for the finite elements, the two systems in a and b are related as follows:

$$v_i^g = B_{ij}^g \rho_j^g \tag{1}$$

$$B_{ji}^g S_j^g = P_i^g \tag{2}$$

Also $(R_i - r_i)$ and $(P_i^g - \rho_i^g)$ systems are related from the kinematic properties of the structure as

$$\rho_i^g = a_{ij}^g r_j \tag{3}$$

Applying the principle of virtual work, the relationship for the nodal forces becomes

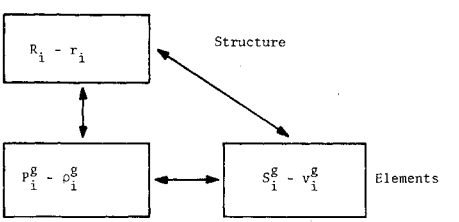


**Fig. 1 Force-displacement system representation of structures.**

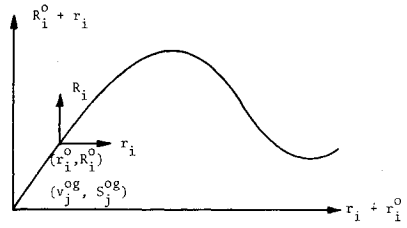


**Fig. 2 Typical load-displacement curve for the large displacement behavior of a structure.**

$$R_i = \sum_g a_{ji}^g P_j^g \tag{4}$$

The incremental equilibrium equations can be defined again for the structure from the principle of virtual work. At a deformed state, generalized stress and strains for each element are defined as $(S_i^{go} - v_i^{go})$ corresponding to load displacement system $(R_i^o, r_i^o)$ for the entire structure, as shown in Fig. 2. The incremental work done by the two systems is as follows:

$$\sum_g (S_i^{go} + S_i^g)\, dv_i^g = (R_j^o + R_j)\, dr_j \tag{5}$$

The nodal forces can then be expressed by a nonlinear incremental relationship as

$$R_j^o + R_j = \sum_g (S_i^{go} + S_i^g) v_{i,j}^g \tag{6}$$

where $v_{i,j}^g = \partial v_i^g / \partial r_j$ is a kinematic relationship depending on the current geometry of the structure. Assuming that the incremental generalized strains $v_i^g$ for the element remain small, the element behavior can be approximated by a linear incremental relationship as

$$S_i^g = k_{ij}^g v_j^g \tag{7}$$

where the element stiffness matrix $k_{ij}^g$ may be a function of $(S_i^{go} - v_i^{go})$. The kinematic nonlinearity in Eq. (6) can be evaluated using a Taylor series expansion of $v_i^g$ in terms of $r_i$ as

$$v_i^g = v_{i,j}^{go} r_j + (1/2!) v_{i,jk}^{go} r_j r_k + (1/3!) v_{i,jkm}^{go} r_j r_k r_m + \cdots \tag{8}$$

and

$$dv_i = v_{i,j}^{go} dr_j + v_{i,jk}^{go} r_k\, dr_j + (1/2!) v_{i,jkm}^{go} r_k r_m\, dr_j + \cdots \tag{9}$$

After defining the arrays $B_{ij}$ and $\Lambda_{ijk}$ as

$$B_{ij}^g = v_{i,j}^{go} \tag{10}$$

$$\Lambda_{ijk}^g = v_{i,jk}^{go} = B_{ij,k}^g \tag{11}$$

and substituting Eqs. (7–9) into Eq. (6), the incremental equilibrium equation can be written as

$$R_j^o + R_j = \sum_g \left\{ B_{ij}^g + \Lambda_{ijk}^g r_k + \frac{1}{2!} \Lambda_{ijk,m}^g r_k r_m + \frac{1}{3!} \Lambda_{ijk,mn}^g r_k r_m r_n + \cdots \right\} \left\{ S_i^o + k_{ij}^g \left[ B_{ij}^g r_j + \frac{1}{2!} \Lambda_{ijk}^g r_j r_k + \frac{1}{3!} \Lambda_{ijk,m}^g r_j r_k r_m + \cdots \right] \right\} \tag{12}$$

By substituting $r_i = 0$ and $R_i = 0$ into Eq. (12) the equilibrium condition at the initial point $(r_i^o, R_i^o)$ can be obtained as

$$R_j^o = \sum_g S_i^{go} v_{i,j}^{go} = \sum_g S_i^{go} B_{ij}^g \tag{13}$$

Dropping the terms in Eq. (13) from Eq. (12), Eq. (12) becomes

$$R_j = \sum_g [B_{ij}^g k_{ik}^g B_{km}^g + S_k^{og} \Lambda_{kjm}^g] r_m + (\text{Higher order terms}) \tag{14}$$

Neglecting the higher terms, Eq. (14) can be expressed in matrix form as

$$\mathbf{R} = \mathbf{K}_T \mathbf{r} \tag{15}$$

where the total incremental stiffness matrix is

$$\mathbf{K}_T = \mathbf{K}_E + \mathbf{K}_G \tag{16}$$

and the elastic stiffness matrix and geometric stiffness matrix are, respectively,

$$\mathbf{K}_E = \sum_g \{B_{im}^g k_{ij}^g B_{jn}^g\} \tag{17}$$

$$\mathbf{K}_G = \sum_g \{S_i^{og} \Lambda_{ijk}^g\} \tag{18}$$

The total incremental stiffness matrix has been employed for buckling analysis of different structures by several authors.[6] The critical or buckling point of a structure can be defined as a point where the incremental displacements $r_i$ can not be determined uniquely from Eq. (15) under an incremental change $R_i = \mu R_i^o$ for the load $R_i^o$. A necessary and sufficient condition for this point of instability is

$$|\mathbf{K}_T| = 0 \tag{19}$$

From a further study of the buckling point of the structure one can also determine whether the buckling is bifurcational or snap-through. In order to obtain a solution for the linearized incremental equilibrium equation at the critical point the augmented matrix $[\mathbf{K}_T \mathbf{R}]$ should have the same rank as $\mathbf{K}_T$. This condition can be satisfied in two ways:

1) The buckling mode is not orthogonal to the loading; but the slope of the generalized load displacement curve is zero ($p_i R_i^o \neq 0$ and $\mu = 0$). $p_i$ is the buckling mode obtained from $\mathbf{K}_T \mathbf{p} = 0$. Then Eq. (15) can be written as

$$\mathbf{K}_T \mathbf{r} = \mathbf{0} \tag{20}$$

and has a solution of $(r_i = \varepsilon p_i)$. The displacements are then in the critical mode. A snap-through type of buckling is obtained.

2) The generalized load displacement curve has a finite slope at the buckling point ($\mu \neq 0$) but the loading is orthogonal to the buckling mode ($p_i R_i^o = 0$). The solution of the incremental equilibrium equation can then be separated into two parts: a general solution and a particular solution as

$$\mathbf{r} = \mu \bar{\mathbf{K}}_T^{-1} \mathbf{R}^o + \delta \mathbf{p} \tag{21}$$

where

$$\bar{\mathbf{K}}_T = \mathbf{K}_T + \zeta \mathbf{p}\, \mathbf{p}^t \tag{22}$$

and $\zeta$ is an arbitrary scalar. In this case the equilibrium path is not unique. As $\zeta$ changes there are an infinite number of solutions. According to the linearized theory, this is a point of neutral equilibrium. In order to determine the possible equilibrium paths, one has to solve higher order equilibrium equations.[1]

## III. Finite Element Analysis for Postbuckling Behavior and Imperfection Sensitivity of Structures

The postbuckling behavior and imperfection sensitivity of structures can be analyzed from the perturbation of the incremental equilibrium equation, Eq. (12), at the buckling point. Following Koiter's analysis, it is assumed that the principal displacements at a point in the neighborhood of the buckling point are in the critical mode $p_i$. Then the displacement vector can be separated into two parts as

$$r_i = \delta p_i + \bar{r}_i \tag{23}$$

where

$$p_i F_{ij} \bar{r}_j = 0 \tag{24}$$

and $F_{ij}$ is an arbitrary positive definite matrix. Substituting Eq. (23) into Eq. (12), and using Eqs. (13) and (19), certain terms can be dropped. The collection of second-order terms in $p_i$ and linear terms in $\bar{r}_i$ yields

$$\mu \mathbf{R}^o = \mathbf{K}_T \bar{\mathbf{r}} + \delta^2 \mathbf{b} \tag{25}$$

where the column vector $\mathbf{b}$ is defined as

$$b_j = \sum_g \Lambda_{ijk}^g p_k k_{im}^g B_{mn}^g p_n + \tfrac{1}{2} B_{ij}^g k_{im} p_n \Lambda_{mnq}^g p_q + \tfrac{1}{2} S_i^{og} \Lambda_{ijk,m}^g p_m p_k \tag{26}$$

By premultiplying the incremental equilibrium equation by the critical mode $p_i$ and then repeating the preceding process, the following equation is obtained:

$$\delta^2 b_i p_i + 2\delta b_i \bar{r}_i + 2\delta^3 A = 0 \tag{27}$$

where

$$A = \sum_g \tfrac{1}{4} p_j \Lambda^g_{ijk} p_k k^g_{im} p_n \Lambda_{mnq} p_q + \tfrac{1}{3} p_j \Lambda^g_{ijk,m} p_k p_m k^g_{in} B^g_{nq} p_q + \tfrac{1}{12} S^{og}_i p_j \Lambda^g_{ijk,mn} p_k p_m p_n \quad (28)$$

Equations (25) and (27) can be used to analyze the postbuckling behavior of structures. The total incremental stiffness matrix $\mathbf{K}_T$ with the geometric stiffness matrices $S^{og}_i \Lambda^g_i$ has been developed for the buckling analysis of different structures in finite element form. Additional matrices to be developed for the postbuckling analysis are primarily $\Lambda^g_{ijk,m}$ and $\Lambda^g_{ijk,mn}$ matrices.

The simultaneous solution of Eqs. (25) and (27) can be used to analyze the bifurcational buckling characteristics in the following manner: a) from the generalized load-displacement curve for $p_i$ displacements where $\mu$ is plotted against $\delta$; b) from the generalized load-displacement curve for $\bar{r}_i$ displacements where $\mu$ is plotted against $R^o_i r_i$. The slope of the curve at the critical point

$$m_1 = \mu/(R^o_i \bar{r}_i) \quad (29)$$

can be compared to the slope of the unbuckled form, to obtain an indication of the change in the stiffness of the structure due to buckling.

### The Analysis of the Fundamental Equilibrium Path

Starting from the unloaded position, the structure follows the fundamental equilibrium path till it reaches the buckling point. The slope of the generalized load-displacement curve for the unbuckled form is

$$m_o = \mu/(R^o_i r^*_i) \quad (30)$$

where $r^*_i$ are the displacements in this mode. $m_o$ can be obtained from the solution of Eq. (31) and from the condition that the path of the unbuckled form must be continuous through the bifurcational point. The incremental equilibrium equation can be written at a point just before the buckling.

$$[\mathbf{K}_T - \varepsilon \mathbf{G}]\mathbf{r}^* = R \quad (31)$$

where $\mathbf{G}$ is a symmetric matrix representing the linearized change in $\mathbf{K}_T$ and $\varepsilon$ is a small scalar. Multiplying by $\mathbf{p}^t$, Eq. (31) becomes

$$\varepsilon \mathbf{p}^t \mathbf{G} \mathbf{r}^* = 0 \quad (32)$$

Therefore, if the path is continuous

$$\mathbf{p}^t \mathbf{G} \mathbf{r}^* = 0 \quad (33)$$

and this condition can be used as a side condition to obtain the postbuckling behavior in the unbuckled mode. Through a modal analysis, it can be shown that the solution of Eqs. (31) and (33) can be obtained from the following equation:

$$\begin{bmatrix} \mathbf{K}_T & \mathbf{p} \\ \mathbf{p}^t & 0 \end{bmatrix} \begin{bmatrix} \mathbf{r}^* \\ \beta \end{bmatrix} = \begin{bmatrix} \mu \mathbf{R} \\ 0 \end{bmatrix} \quad (34)$$

### The Analysis of the Buckled Equilibrium Path

Inspection of Eqs. (25) and (27) show that if the coefficient of the $\delta^2$ term in Eq. (27) is zero, then the solution has two symmetric roots. A symmetric bifurcation point can be defined from this condition as

$$b_i p_i = 0 \quad (35)$$

Physically, this condition shows that the second-order forces resulting from the linear displacements in the buckling mode do no work on the critical mode itself. Consequently, Eqs. (25) and (27) can be written as

$$\begin{bmatrix} \mathbf{K}_T & \mathbf{b} \\ \mathbf{b} & A \end{bmatrix} \begin{bmatrix} \bar{\mathbf{r}} \\ \delta^2 \end{bmatrix} = \mu \begin{bmatrix} \mathbf{R}^o \\ 0 \end{bmatrix} \quad (36)$$

This system has a unique solution under the condition, $p_i F_{ij} \bar{r}_j = 0$. Through a modal analysis it can be shown that the solution of these equations can be obtained as follows:

$$\delta^2/\mu = (\mathbf{b}^t \bar{\mathbf{K}}_T^{-1} \mathbf{R}^o)/(\mathbf{b}^t \bar{\mathbf{K}}_T^{-1} \mathbf{b} - A) \quad (37)$$

$$m_1/m_o = 1 + (\delta^2/\mu)[(\mathbf{b}^t \mathbf{r}^*)/(\bar{\mathbf{r}}^t \mathbf{R}^o)] \quad (38)$$

Equations (37) and (38) can be used to determine whether the critical point is stable or unstable.

The definition of the asymmetric bifurcation is similar to the definition of symmetric bifurcational buckling. If the condition of orthogonality is not satisfied for $\mathbf{b}$ and $\mathbf{p}$ matrices

$$b_i p_i \neq 0 \quad (39)$$

the postbuckling behavior is asymmetric. The equilibrium equations can then be written as

$$\mathbf{K}_T \bar{\mathbf{r}} + \delta^2 \mathbf{b} = \mu \mathbf{R} \quad (40)$$

$$\tfrac{1}{2}\delta^2 \mathbf{b}^t \mathbf{p} + \delta \mathbf{b}^t \bar{\mathbf{r}} + \delta^3 A = 0 \quad (41)$$

or

$$\begin{bmatrix} \mathbf{K}_T & \mathbf{b} \\ \mathbf{b}^t & A \end{bmatrix} \begin{bmatrix} (\bar{\mathbf{r}} + \frac{1}{2}\delta \mathbf{p}) \\ \delta^2 \end{bmatrix} = \mu \begin{bmatrix} \mathbf{R}^* \\ 0 \end{bmatrix} \quad (42)$$

From the solution of Eq. (42), $\delta$ can be determined as

$$\delta = [2p_i(\bar{r}_i + \tfrac{1}{2}\delta p_i)]/(p_i p_i) \quad (43)$$

Premultiplying Eq. (40) by $\mathbf{p}$, and using Eq. (39), it can be shown

$$\delta^2 = 0 \quad (44)$$

Therefore, only a linear postbuckling variation can be obtained in this case. It is also important to note that $A$ is not required for the solution.

A comparison of the equations for the buckled and unbuckled forms

$$\mathbf{K}_T \bar{\mathbf{r}} = \mu \mathbf{R}^o \qquad \mathbf{p}^t \bar{\mathbf{r}} = 0 \quad (45)$$

$$\mathbf{K}_T \mathbf{r}^* = \mu \mathbf{R}^o \qquad \mathbf{b}^t \mathbf{r}^* = 0 \quad (46)$$

shows that buckled and uncoupled shapes differ only in the buckling mode. Therefore, the slope of the generalized postbuckling curve in the $(\mu - R_i \bar{r}_i)$ plane does not change according to this analysis.

### The Analysis of the Imperfection Sensitivity of Structures

The effect of imperfections on the stability of structures can be calculated in a general form from the developed postbuckling analysis. A generalized displacement function is defined at the critical point as

$$r_i = \delta p_i + \bar{r}_i + \gamma_i \quad (47)$$

where $\gamma_i$ represents the initial imperfections for the structure. The incremental equilibrium equations for structures, with symmetric bifurcation points and initial imperfections $\gamma_i$, can be written as

$$\mu \mathbf{R}^o = \mathbf{K}_T \bar{\mathbf{r}} + \delta^2 \mathbf{b} + \mathbf{K}_E \boldsymbol{\gamma} \quad (48)$$

$$2\delta^3 A + 2\delta \mathbf{b}^t \bar{\mathbf{r}} - \mathbf{p}^t \mathbf{K}_E \boldsymbol{\gamma} + \sum_g \tfrac{1}{2} B^g_{ij} p_j k^g_{im} \gamma_n \Lambda^g_{mnq} \gamma_q - \tfrac{3}{2}\delta B^g_{ij} p_j k^g_{im} p_n \Lambda^g_{mnq} p_q = 0 \quad (49)$$

In order to analyze the effect of the imperfections on the solution of these equations, the imperfection vector can be separated into two components

$$\gamma_i = \varepsilon q_i + \beta p_i \quad (50)$$

under the orthogonality condition

$$\mathbf{p}^t \mathbf{K}_E \mathbf{q} = 0 \quad (51)$$

The following limitations on the magnitude of these two types of imperfections must be imposed in order to obtain a consistent solution of the incremental equilibrium equations

$$\varepsilon < \delta^{3/2} \quad \text{and} \quad \beta < \delta^3 \quad (52)$$

Substituting Eqs. (48, 50, and 51) into Eq. (49), the maximum value of $\mu$ can be obtained from this equation, which represents the snap-through behavior of the imperfect structure at the critical point. For symmetric bifurcational buckling separating the imperfections into two parts, the drop in the critical load due to an imperfection is as follows:

$$\lambda_d = -\varepsilon \left( b_i s_i + \sum_g \tfrac{3}{4} B^g_{ji} p_i k^g_{jk} p_m \Lambda^q_{kmn} p_n \right) \Big/ b_i t_i - 3(A - b_i u_i)/(b_i t_i)[(\beta \mathbf{p}^t \mathbf{K}_E \mathbf{p} + \tfrac{1}{2}\varepsilon^2 B^g_{ij} k^g_{jk} q_m \Lambda^g_{kmn} q_n)/4(A - b_i u_i)]^{2/3} \quad (53)$$

where

$$\mathbf{s} = \bar{\mathbf{K}}_T^{-1} \mathbf{K}_E \mathbf{q} \quad (54)$$

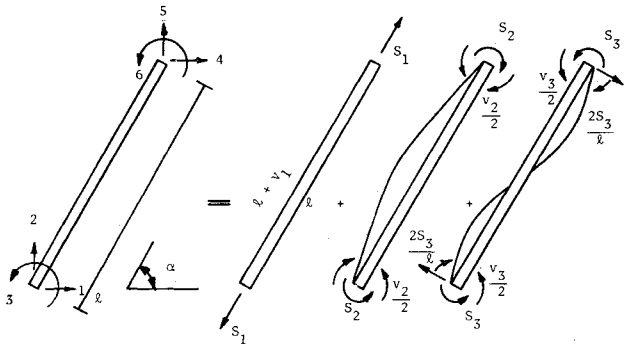

Fig. 3 Geometry and generalized stress-strain system of a beam-column element.

$$\mathbf{t} = \bar{\mathbf{K}}_T^{-1}\mathbf{R}^o \tag{55}$$

$$\mathbf{u} = \bar{\mathbf{K}}_T^{-1}\mathbf{b} \tag{56}$$

Using Eq. (38), the preceding expression simplifies to

$$\lambda_d = -\varepsilon\left[\left(b_i s_i + \sum_g \tfrac{3}{4}B_{ji}^g p_i k_{jk}^g q_m \Lambda_{kmn}^g q_n\right)\Big/(b_i t_i)\right] - 3\frac{\mu}{\delta^2}\delta_1^2 \tag{57}$$

where $\delta_1$ is the magnitude of the displacements in the critical mode $p_i$ at the new critical point and can be determined as

$$\delta_1^3 = \left(\beta \mathbf{p}^t \mathbf{K}_E \mathbf{p} + \sum_g \tfrac{1}{2}\varepsilon^2 B_{ji}^g p_i k_{jk}^g q_m \Lambda_{kmn}^g q_n\right)\Big/[4(A - b_i u_i)] \tag{58}$$

The postbuckling slope of the perfect structure is an important factor for the imperfection sensitivity of structures due to imperfections in the critical mode, as can be seen from Eq. (57).

For asymmetric structures with imperfections, the equilibrium equations are formulated under the assumptions

$$\varepsilon < \delta \qquad \beta < \delta^2 \tag{59}$$

The drop in the critical load can be written in this case as

$$\lambda_d = [(\tfrac{3}{4}B_{ji}^g p_i k_{jk}^g p_m \Lambda_{kmn}^g p_n + b_i s_i)/b_i t_i] - (\mu/\delta)\,\delta_1 \tag{60}$$

where

$$\delta_1^2 = \left(-\beta \mathbf{p}^t \mathbf{K}_E \mathbf{p} + \sum_g \tfrac{1}{2}\varepsilon^2 B_{ij} p_j k_{ik} q_m \Lambda_{kmn} q_n\right)\Big/ b_i p_i \tag{61}$$

From the analysis of Eqs. (57) and (60) the imperfections in the buckling mode of the structure are important in determining the buckling load of the imperfect structure. The buckling is of a snap-through type and the buckling load is lower in magnitude. Only for certain symmetric structures this is not the case. For example, a symmetric arch with an asymmetric critical mode still displays a bifurcational buckling behavior for symmetric imperfections. The imperfections orthogonal to the critical mode have a second-order effect.

## IV. Application of the Method: Postbuckling Analysis of Arches

A family of two-hinged arches is analyzed to demonstrate the generality of the method. A funicular arch was selected so that the prebuckling deformations remain small and can be neglected. It was assumed that the members are straight at the buckling point and the initial forces are only axial. A complete parabolic arch was used to obtain symmetric bifurcation points. By changing merely the width/span ratio, stable and unstable bifurcation points were obtained. Another particular arch with an asymmetric geometry was used to obtain asymmetric bifurcation points. The numerical procedure can be summarized in the following order: a) derivation of the finite element; b) formulation of the necessary matrices required for the solution of postbuckling equations; c) solution of the system of equations.

The finite element model used for the postbuckling analysis of arches is a beam-column element, as shown in Fig. 3. The element nodal force-displacement system $(P_i^g - \rho_i^g)$ is defined

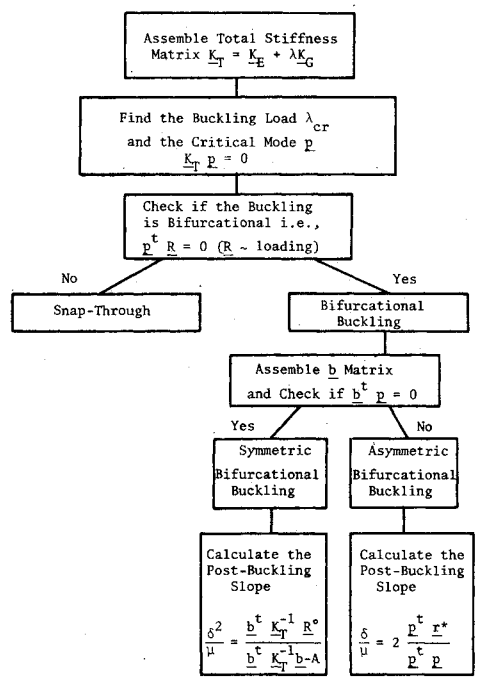


Fig. 4 Flow chart for the mathematical analysis of the postbuckling behavior of structures.

$$\mathbf{P}^g = \{P_i^g\}, \quad i = 1, 6 \tag{62}$$

and

$$\boldsymbol{\rho}^g = \{\rho_i^g\}, \quad i = 1, 6 \tag{63}$$

Element strains and stresses can be described by the three generalized stress-strain relationships $(S_i^g - V_i^g)$, as also shown in Fig. 3. In this case $B_{ij}^g$ can be derived from the statical or kinematical relationship as

$$\{B_{ij}^g\} = \begin{bmatrix} -\cos\alpha & -\sin\alpha & 0 & \cos\alpha & \sin\alpha & 0 \\ 0 & 0 & 1 & 0 & 0 & -1 \\ -\dfrac{2\sin\alpha}{l} & \dfrac{2\cos\alpha}{l} & 1 & \dfrac{2\sin\alpha}{l} & -\dfrac{2\cos\alpha}{l} & 1 \end{bmatrix} \tag{64}$$

The linear elastic stiffness matrix for the element is

$$\{k_{ij}^g\} = \frac{E}{l}\begin{bmatrix} A & 0 & 0 \\ 0 & I & 0 \\ 0 & 0 & 3I \end{bmatrix} + S_{io}\begin{bmatrix} 0 & 0 & 0 \\ 0 & \dfrac{l}{12} & 0 \\ 0 & 0 & \dfrac{l}{20} \end{bmatrix} \tag{65}$$

$\Lambda_{ij}$, $\Lambda_{ijk,m}$, and $\Lambda_{ijk,mn}$ matrices are derived from Eq. (11) using the $B_{ij}^g$ matrix in Eq. (64). The numerical procedure for the postbuckling analysis is summarized in a flow chart in Fig. 4. The two arches used to obtain symmetric and asymmetric bifurcation points are shown in Fig. 5. They represent two

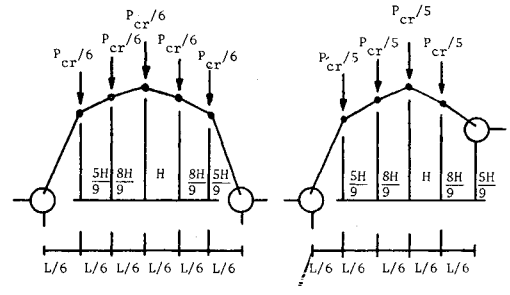


Fig. 5 Geometry and loading of the symmetric and asymmetric arches for sample cases.

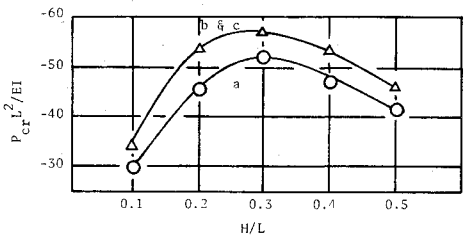


**Fig. 6 Variation of buckling loads for a symmetric arch with $H/L$ ratios.**

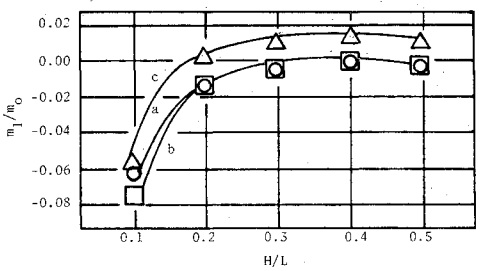


**Fig. 8 Comparison of the prebuckling and postbuckling stiffnesses of a symmetric arch.**

discretized models of a parabolic arch carrying a total vertical load $P$, distributed uniformly over the span $L$. Numerical values for $I/AL^2$ were chosen so that bifurcational buckling was obtained. The critical loads obtained from the eigenvalue analysis are illustrated in Fig. 6 for a symmetric arch.

Five different $H/L$ ratios were tested. For these different cases the effect of derivatives of $\Lambda_{ijk}$ matrices were considered. The results were illustrated in Figs. 7 and 8 showing the five values for each case obtained a) by complete formulation of the method including the influence of element axial forces on bending in Eq. (64); b) without element axial force corrections; c) without the correction terms and the derivatives of $\Lambda_{ijk}$ matrices, by using only second-order kinematic relations.

Analyses of these results show that shallow arches display unstable bifurcation points while high arches are slightly stable. Another important observation is that the derivatives of $\Lambda_{ijk}$ matrices do not have a major effect on the postbuckling slope of shallow arches; whereas, for high arches the change in $\delta^2/\mu$ and $m_1/m_o$ is quite important. In addition, the results also indicate that the correction of the element stiffness matrices improves the accuracy of the buckling load, while the postbuckling characteristics do not change significantly. Finally, these results show that as the number of elements increase, the accuracy of the calculations without the axial force correction terms improves considerably.

The arches used to obtain asymmetric bifurcation points were obtained from symmetric arches by removing an element from the right-hand side of the arch, as shown in Fig. 5. The results for different $H/L$ values are given in Figs. 9 and 10. In this case the postbuckling curve for the deflection $\delta$ has a definite slope at the critical point and this slope decreases for higher arches.

A comparison of the postbuckling behavior and imperfection sensitivity of the symmetric and asymmetric arches discussed in this paper can be made by plotting the magnitude of the eigenvalue displacements $\delta p_i$ against the load increment $\mu$. Such results are shown in Fig. 11. Compared to the symmetric arch, the asymmetric arch has a considerably higher critical load; but the postbuckling slope is steeper and therefore the structure is more sensitive to imperfections. This argument also implies that the prebuckling deformations may cause an important decrease in the buckling load of an asymmetric arch.

## V. Other Applications: Columns and Plates

With the finite element formulation, the postbuckling behavior of a column under axial deformations can be solved using the same numerical technique developed for the analysis of arches. Since the critical mode of a column has a sine curve, it is possible to derive a set of difference equations and obtain an analytical solution for the finite element model of a column. This analytical solution is useful to explain the numerical errors and to show the effects of the higher order terms in the equilibrium equations.

The buckling load of a column can be written as

$$P = [(12EI)/L^2)][(n^2 \sin^2 \Pi/4n)/(3 - 2\sin^2 \Pi/4n)] \quad (66)$$

where $n$ is the number of finite elements representing the column of length $L$. The postbuckling slope of the column is found

$$\delta^2/\mu = [(2L^2)/(n^2 \sin^2 \Pi/4n)][(1 + P/EA)/(1 + 3P/EA)] \quad (67)$$

The convergence of these results for increasing number of elements is shown in Fig. 12. These results show that the postbuckling slope is less sensitive to discretization errors than the buckling load.

For an incompressible column, if the $\Lambda_{ijk,m}$ and $\Lambda_{ijk,mn}$ terms are neglected, the postbuckling slope becomes

$$\delta^2/\mu = -(16L^2)/(3\Pi^2) \quad (68)$$

Equation (68) indicates an unstable postbuckling behavior for a column and is obviously in error. This result together with the result obtained for arches indicates that these higher order terms are important when the postbuckling slope of the structure is relatively small. The same idea can be used in determining the postbuckling behavior of plates.

The postbuckling behavior of plates has long been a popular subject,[14] due to certain simplifications in the formulation of

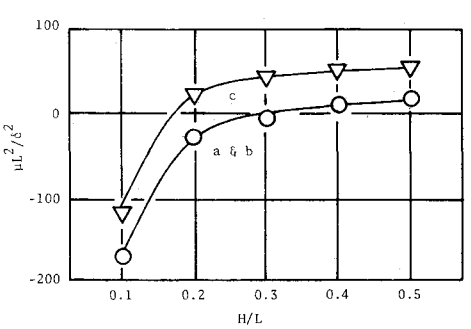


**Fig. 7 Slope of the postbuckling deflections of a symmetric arch in the buckling mode.**

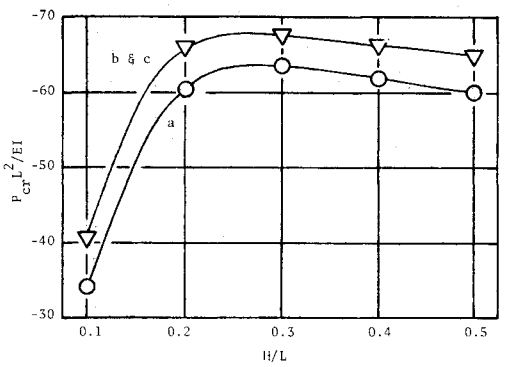


**Fig. 9 Variation of buckling loads for an asymmetric arch with $H/L$ ratios.**

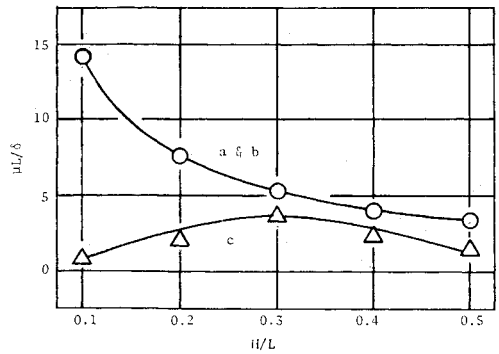


**Fig. 10 Slope of postbuckling deflections on an asymmetric arch in the buckling mode.**

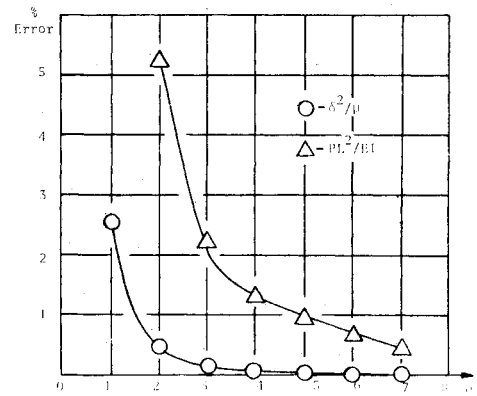


**Fig. 12 Variation of errors in the calculated buckling load and postbuckling slope of a column with varying number of elements.**

the large-displacement analysis of plates. In the context of the finite element method, these simplifications involve neglecting $\Lambda_{ijk,m}$ and $\Lambda_{ijk,mn}$ terms and dropping some of the $\Lambda_{ijk}$ matrices. The axial and in-plane displacements can be separated as in the case of column and do not contain in-plane displacements. The postbuckling behavior of plates can be analyzed by the presented general method. Since $p_i b_i = 0$, these structures produce symmetric bifurcation points. Dropping the higher order terms,

$$b_i = \sum_g \Lambda^g_{jik} p_k k^g_{im} B^g_{mn} p_n + \tfrac{1}{2} B^g_{ji} k^g_{jk} p_n \Lambda^g_{kmn} p_n \qquad (69)$$

and

$$A = \sum_g p_j \Lambda^g_{ijk} p_k k^g_{im} p_n \Lambda^g_{mnq} p_q \qquad (70)$$

Sample numerical results for plates are shown in Fig. 13. As can be seen from Eqs. (69) and (70), the analysis requires no additional matrices other than the ones for buckling analysis. The results are quite accurate. The application of the finite element method enables the analysis of plates with arbitrary boundary conditions.

## VI. Conclusions

The developed method deals with the finite element analysis of the elastic instability of structures in a general manner. As described in the analysis, the buckling and postbuckling characteristics of a structure and its imperfection sensitivity can be evaluated in a unified manner, based on its finite element model.

The applicability of the method for different structures was demonstrated by analyzing the postbuckling behavior of arches. The analysis of plates showed that for structures with a first-order postbuckling stiffness, the numerical procedure can be simplified by dropping the higher order terms corresponding to the derivatives of geometric stiffness matrices. The analysis of columns indicated the magnitude of the involved numerical errors and showed that the accuracy of the results for the postbuckling analysis were comparable to the accuracy of the buckling loads. The method can be applied for any structure by deriving the higher order geometric stiffness matrices. Also, the presentation of the method gives an insight for deciding the governing terms in the geometric stiffness matrices. Depend-

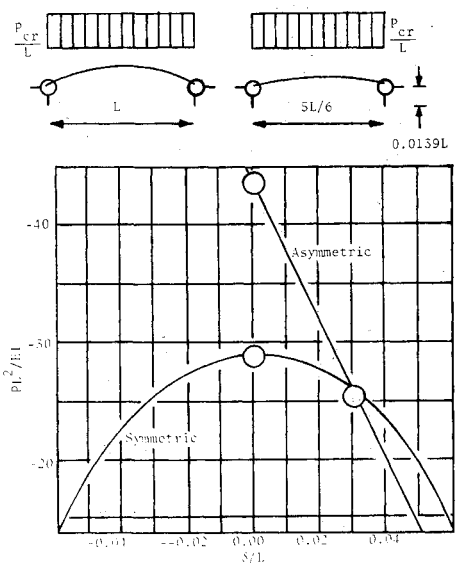


**Fig. 11 Comparison of the postbuckling behavior of a symmetric and an asymmetric arch.**

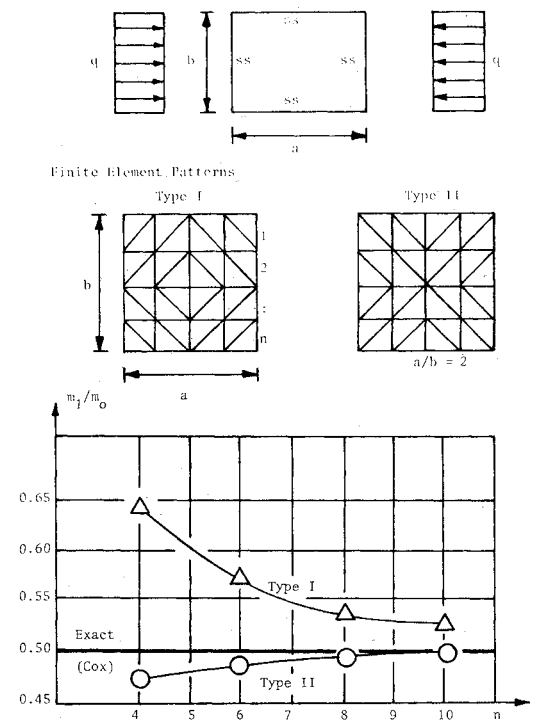


**Fig. 13 Postbuckling behavior of a simply-supported square plate loaded in its plane. (Four edges remain straight.)**

ing on the geometry and loading of the structure, only a portion of higher order geometric stiffness matrices is required for obtaining an approximate but accurate result.

## References

[1] Koiter, W. T., "The Stability of Elastic Equilibrium," thesis, 1945, Polytechnic Inst. at Delft, Amsterdam; English translation AFFDL-TR-70-25, 1970, Air Force Flight Dynamics Lab., Wright-Patterson Air Force Base, Ohio.

[2] Sewell, M. J., "A Method of Post-Buckling Analysis," *Journal of Mechanics and Physics of Solids*, Vol. 17, 1969, pp. 217–233.

[3] Thompson, J. M. T., "Basic Principles in the General Theory of Elastic Stability," *Journal of Mechanics and Physics of Solids*, Vol. 11, 1963, pp. 13–20.

[4] Budiansky, B. and Hutchinson, J. W., "Dynamic Buckling of Imperfection Sensitive Structures," *Proceedings of the XIth International Congress of Applied Mechanics*, edited by H. Goertler, Springer-Verlag, Berlin, 1966, pp. 636–651.

[5] Lang, T. E., "Post-Buckling Response of Structures Using the Finite Element Method," Ph.D. dissertation, 1969, Univ. of Washington, Seattle, Wash.

[6] Mallett, R. H. and Marcal, P. V., "Finite Element Analysis of Nonlinear Structures," *Journal of the Structural Division, ASCE*, Vol. 94, No. ST9, Sept. 1968, pp. 2081–2105.

[7] Murray, D. W. and Wilson, E. L., "Finite Element Postbuckling Analysis of Thin Elastic Plates," *AIAA Journal*, Vol. 7, No. 10, Oct. 1969, pp. 1915–1920.

[8] Mak, C. K. and Kao, D.-W., "Finite Element Analysis of Buckling and Post-Buckling Behaviors of Arches with Geometric Imperfections," *Computer and Structures*, Vol. 3, No. 1, Jan. 1973, pp. 149–161.

[9] Tong, P. and Pian, T. H. H., "Post-Buckling Analysis of Shells of Revolution by the Finite Element Method," Symposium on Thin Shell Structures, California Inst. of Technology, Pasadena, Calif., June 29–30, 1972.

[10] Gallagher, R. H., Lien, S., and Mau, S. T., "A Procedure for Finite Element Plate and Shell Pre- and Post-Buckling Analysis," Air Force 3rd Conference on Matrix Methods in Structural Mechanics, Wright-Patterson Air Force Base, Ohio, Oct. 1971.

[11] Mallett, R. J. and Haftka, R. T., "Progress in Nonlinear Finite Element Analysis Using Asymptotic Solution Techniques," *Advances in Computational Methods in Structural Mechanics and Design*, edited by J. T. Oden, R. W. Clough, and Y. Yamamoto, UAH Press, Univ. of Alabama in Huntsville, 1972, pp. 357–373.

[12] Martin, H. C., "On the Derivation of the Stiffness Matrices for the Analysis of Large Deflection and Stability Problems," *Proceedings, Conference on Matrix Methods in Structural Mechanics*, edited by J. S. Przemieniecki, AFFDL-TR-66-80, Wright-Patterson Air Force Base, Ohio, 1966.

[13] Argyris, J. H., Kelsey, S., and Kamel, H., "Matrix Methods of Structural Analysis—A Precis of Recent Developments," *Matrix Methods in Structural Analysis*—AGARDograph 72, edited by B. Fraeijs de Veubeke, Pergamon Press, Oxford, 1964, pp. 1–164.

[14] Cox, H. L., *The Buckling of Plates and Shells*, Macmillan, New York, 1963.